# Combining Pattern, Polarization and Channel Balance Correction Routines to Improve the Performance of Broad Band, Dual Polarized Probes

Patrick Pelland, Allen Newell
Nearfield Systems Inc.
19730 Magellan Drive,
Torrance, CA 90502-1104

***Abstract* - Broad band, dual polarized probes are becoming increasingly popular options for use in near-field antenna measurements. These probes allow one to reduce cost and setup time by replacing several narrowband probes like open-ended waveguides (OEWG) with a single device covering multiple waveguide bands. These probes are also ideal for production environments, where chamber throughput should be maximized. Unfortunately, these broadband probes have some disadvantages that must be quantified and corrected for in order to make them viable for high accuracy near-field measurements. Most of these broadband probes do not have low cross polarization levels across their full operating bandwidths and may also have undesirable artifacts in the main component of their patterns at some frequencies. Both of these factors will result in measurement errors when used as probes. Furthermore, the use of a dual port RF switch adds an additional level of uncertainty in the form of port-to-port channel balance errors that must be accounted for. This paper will describe procedures to calibrate the pattern and polarization properties of broad band, dual polarized probes with an emphasis on a newly developed polarization correction algorithm. A simple procedure to measure and correct for amplitude and phase imbalance entering the two ports of the near-field probe will also be presented. Measured results of the three calibration procedures (pattern, polarization, channel balance) will be presented for a dual polarized, broad band quad-ridged horn antenna. Once calibrated, this probe was used to measure a standard gain horn (SGH) and will be compared to baseline measurements acquired using a good polarization standard OEWG. Results with and without the various calibration algorithms will illustrate the advantage to using all three routines to yield high accuracy far-field pattern data.**

**Keywords:** near-field, measurements, spherical, near-field probe calibration, polarization, channel balance.

## I. INTRODUCTION

In order to accurately compute the far-field pattern of an antenna resulting from a near-field measurement, knowledge of the probe's radiation pattern is required. Without this information, the results of the near-field to far-field transformation will be a combination of the responses of the probe and antenna under test (AUT). When the probe's pattern is known, one can correct for its contribution and isolate the response of the AUT. Once the AUT's radiation pattern has been computed, a variety of useful parameters can be extracted (directivity, beam peak direction, phase center location, polarization, etc.).

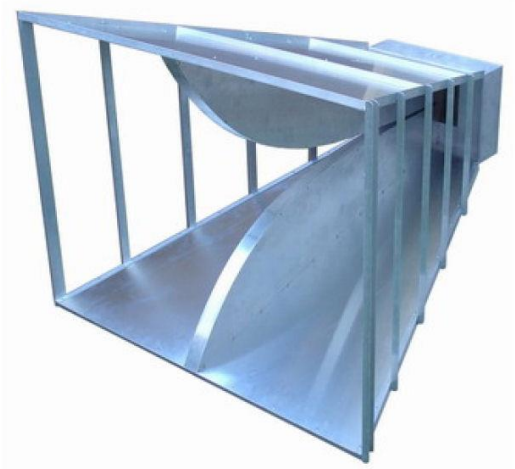

Figure 1. NSI-RF-RGP-200 Broadband Dual-Ridged Horn (DRH)

In order to simplify the probe correction process, a common practice is to utilize antennas that can be easily modeled using reference to industry standard antenna design literature. The most popular choice is the open-ended waveguide (OEWG) probe, which is used extensively in near-field antenna measurements. These low-cost probes can be modeled very accurately, which eliminates the need for calibration for the majority of test applications. They also have low on-axis cross-polarization levels (more than 50 dB below the main component), which is beneficial for the probe correction process. However, they are narrow band devices and contain a single RF feed point, meaning that the probe

must be rotated by 90 degrees to acquire dual polarized far-field data.

To increase the efficiency of near-field test systems, broad band probes like the dual-ridged horn in Figure 1 are sometimes used. These probes can cover several OEWG bands which greatly reduces the amount of system re-configuration required. The dual-ridged horn (DRH) probe shown in Figure 1 is also considerably smaller than an OEWG probe operating at its lowest frequency in the VHF range. Since these probes do not radiate as predictably as a function of frequency as their OEWG alternatives, they must be characterized before use. Once a probe has been characterized, it can be used as near-field probe for future measurements and its response can be de-coupled from the AUT's response using the probe correction process. Some guidelines regarding the probe's directivity, polarization properties and cross-polarization levels should also be established before selecting a particular broad band probe for use in near-field measurements.

Figure 2. NSI-RF-DPP-50 Broad Band Quad-Ridged Horn (QRH)

In order to further reduce total test time for production environments, dual polarized, broad band probes are often used. One such probe is the quad-ridged horn shown in Figure 2. While these probes have the potential to dramatically increase system throughput, they present an additional level of complexity and cost over probes with a single RF excitation port. Firstly, they require the use of an RF switch to excite both ports. The amplitude and phase entering either port through the switch and cable network will not be identical. If not accounted for, this fact will result in far-field pattern errors. Secondly, for the spherical near-field (SNF) geometry (which is of primary interest here), the transformation from near-field to far-field requires that the two ports of the probe have identical far-field patterns (rotated by 90 degrees). Dual polarized probes are designed with this in mind, but manufacturing tolerances and mechanical non-symmetries can lead to pattern differences between the two ports. In addition, many of these antennas have poor cross-polarization levels like the dual log periodic probes discussed in [1]. See TABLE I for a summary of the probes discussed in this section.

TABLE I. COMPARISON OF VARIOUS LINEARLY-POLARIZED PROBES DISCUSSED IN THIS PAPER

| Type | OEWG | DRH | QRH |
|---|---|---|---|
| **Cost** | Low | High | Very High[1] |
| **Bandwidth** | Narrow | Broad | Broad |
| **Meas. Time** | 2x | 2x | 1x |
| **Calibration Required** | None | Pattern | Pattern, Polarization, Channel Balance |

[1] The QRH probe also requires the use of an RF switch to excite both ports, increasing total cost.

This paper will present a continuation of the research started in [1] and expanded upon in [2] by focusing on improving the performance of broad band, dual polarized probes in SNF measurements. It will be shown that by using pattern, polarization and channel balance correction good performance can be achieved using these probes. Each of the correction algorithms will be presented, followed by some validation measurements on a standard gain horn (SGH) antenna.

## II. Probe Pattern Correction

Prior to selecting any antenna for use as probe in near-field measurements, an accurate understanding of the probe's radiation pattern is required. In theory, without knowledge of the probe's pattern, it is not possible to accurately isolate the response of the AUT from the response of the probe, meaning the far-field results will be an unknown combination of the two responses.

The OEWG antenna is well-suited for near-field measurements since we can accurately predict the probe's radiation properties without the need to measure it in an antenna test range. These antennas also have low on-axis cross-polarization levels and broad main component patterns, leading to small measurement errors related to the probe, namely:

1. Probe relative pattern errors.
2. Probe polarization errors.
3. Probe misalignment errors. [9,10]

For SNF systems, ignoring the effects of the probe (considering it as an isotropic radiator) can sometimes leads to negligible or small errors in the main beam response of the AUT. Since OEWG probes have broad main beam patterns, the region illuminating the AUT often appears to be an isotropic radiator, provided the AUT is not very large or offset a large distance from the measurement origin. Figure 3 shows a comparison of

measured directivity for a WR187 standard gain horn using a WR187 OEWG probe. There is virtually no difference in peak directivity calculations with and without probe correction enabled. Both responses are shown overlaid with the theoretical directivity of this antenna. The same exercise is completed using a QRH probe measuring the same WR187 SGH, with results presented in Figure 4. Since the QRH probe is considerably more directive than the OEWG alternative, large errors in AUT directivity arise when we ignore probe correction (assume the probe is an isotropic radiator). When probe correction is applied, the results agree very well with the theoretical calculation and we also see the real periodic variations of an SGH.

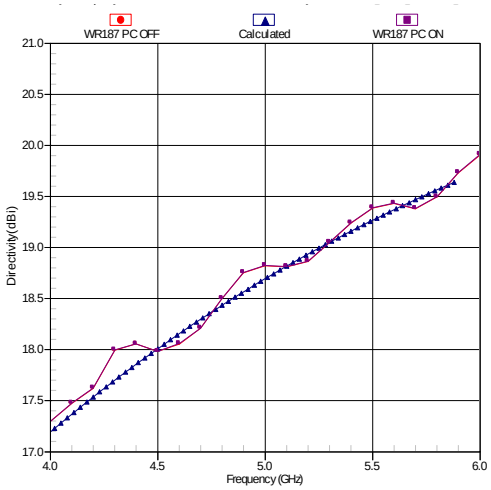


Figure 3. WR187 Standard Gain Horn Measured with WR187 OEWG Probe showing Negligible Effect of Probe Pattern Correction on Directivity

When an interest in reducing test time arises, we start to consider broad band and dual polarized antennas like the one described above to be used as near-field probe. Unfortunately, these antennas have some disadvantages over the OEWG standard previously discussed. Firstly, the directivity of these antennas tend to vary more as a function of frequency than the OEWG probes whose directivity increase smoothly as a function of frequency. Secondly, the cross-polarization levels of these antennas can sometimes be very high relative to the main component.

Prior to using one of these antennas as a probe in a near-field test system, it should be characterized so that its response can be included as probe correction in the near-field to far-field transformation. The probe characterization should, if possible, be performed in a calibration laboratory with a traceable calibration report. When this is not an option, the chosen facility should at least be able to demonstrate that measurement uncertainty levels are within acceptable limits using a measurement uncertainty evaluation like the NIST 18-term error analysis technique presented in [3,6,7,8]. It is also important to characterize the antenna at many frequency points to avoid the need for future pattern interpolation in the probe correction process.

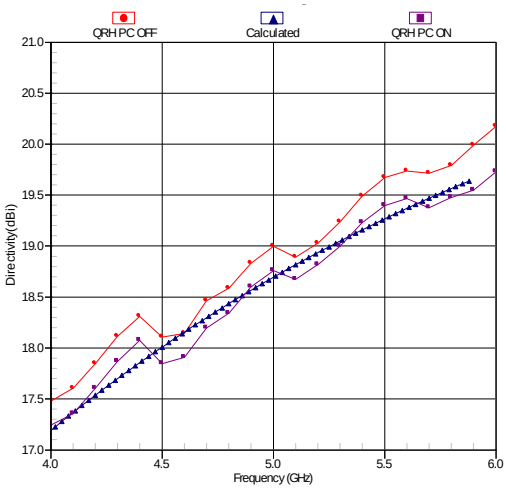


Figure 4. WR187 Standard Gain Horn Measured with DRH Probe showing Impact of Probe Pattern Correction on Measured Directivity

For the purposes of this paper, the QRH antenna shown in Figure 2 was selected to be used as a near-field probe. Before use, it was characterized across its band using a series of OEWG probes. One of the test configurations in the WR28 band (26.5 – 40 GHz) is shown in Figure 5, where the QRH antenna is mounted as AUT and the WR28 OEWG probe is being used to measure its response. Measurements were completed using the Theta-over-Phi swing arm type spherical near-field scanner outlined in TABLE II. The QRH was measured at very fine frequency spacing to minimize errors associated with probe pattern interpolation. Both ports of the antenna are measured across the entire band, although probe pattern correction is implemented based on the first port (E-field along X-axis at $\phi=0°$) of the probe only. Data for the second port of the probe (E-field along Y-axis at $\phi=90°$) is used for the polarization correction described in the next section.

TABLE II. NEAR-FIELD TEST SYSTEM USED FOR PROBE CHARACTERIZATION AND VALIDATION MEASUREMENTS

| | |
|---|---|
| **Measurement Geometry** | Spherical Near-Field |
| **Scanner Model** | NSI 700S-85 Theta-over-Phi |
| **Antenna Under Test** | WR28 & WR62 SGH |
| **Positioner Controller** | NSI Panther Motion Controller |
| **Receiver** | NSI Panther 9000 |

Figure 6 shows the QRH probe's H-Plane pattern at several frequencies across the WR28 band. The peak directivity changes by approximately 3 dB over these

frequencies. Without probe correction data, some directivity error like what was observed in Figure 4 may result.

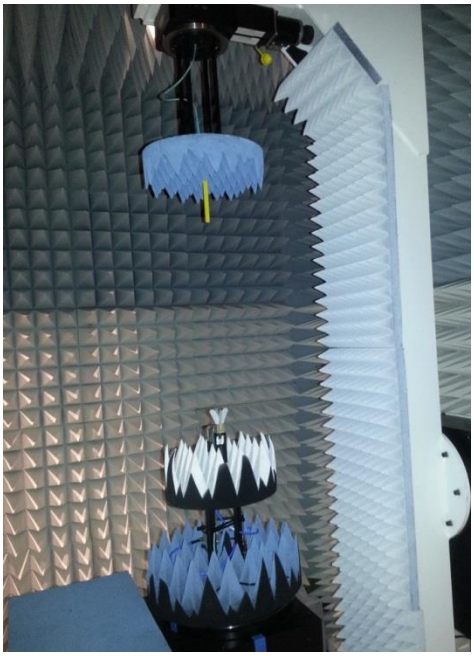

Figure 5. Characterizing the Quad-Ridged Horn on the NSI Spherical Near-Field System

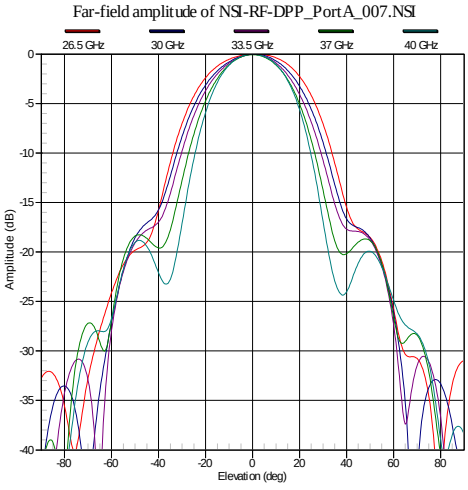


Figure 6. H-Plane Pattern of the QRH's X-Port at Select Frequencies

## III. Polarization Correction Routine

In SNF measurements, a single linearly polarized probe is typically used and the theory assumes that the probe is rotated by 90 degrees to acquire the second polarization. Probe correction using two complete sets of probe coefficients for different patterns is not permitted and so data is provided for a single linearly polarized probe. Because of this fact, a good dual polarized probe should have two ports that appear to be identical, with the second of the two ports appearing to be a rotated version of the first port. Since this is not always the case in practice, dual polarized probes may introduce additional measurement uncertainty, usually quite noticeable in the far-field results of the AUT's cross-polarized component. In order to improve the ability of these dual polarized probes to accurately measure and calculate the cross-polarization levels of an AUT, we introduce a polarization correction factor.

The polarization correction begins during the probe characterization stage. While the mode coefficients used in probe correction are based on the X-port of the probe, both ports should be measured so that the polarization properties of both ports can be extracted. Once complete, the axial ratios, tilt angles and senses of polarization for both ports of the probe are calculated and recorded. The equations shown below for the X-Port are then used to convert these parameters to complex ratios for the circular and linear polarization ratios. The same ratios are calculated for the probe's Y-port.

$$|\rho_{cx}| = \frac{L_x}{R_x} = \frac{AR_x - 1}{AR_x + 1} \text{ if Sense} = \text{Right}$$

$$= \frac{AR_x + 1}{AR_x - 1} \text{ if Sense} = \text{Left}$$

$$ARG(\rho_{cx}) = -2\tau_x$$

$$\rho_{Lx} = \frac{i(\rho_{cx} + 1)}{\rho_{cx} - 1}$$

*Where*

$\rho_{cx}$ = Circular polarization ratio for the X-Port of the probe

$\rho_{Lx} = \frac{AZ_x}{EL_x}$ = Linear polarization for the X-Port of the probe

$AR_x$ = Axial ratio for the X-Port of the probe

$\tau_x$ = Title angle for X-Port of the probe

Probe pattern files are created from pattern measurements on the X-port of the probe. Spherical near-field measurements are performed on an AUT using the two ports of the probe. Below, the data measured by the X-Port is denoted $B_x\ (\theta,\varphi)$ and the data measured by the Y-Port is denoted $B_y\ (\theta,\varphi)$. The Y-Port data is corrected using the following equation to make it equal the data that would have been measured by the rotated X-Port using the following equation:

$$B_{yCorr} = \frac{-B_x(\theta,\phi)\left(\frac{1}{\rho_{Lx}} + \rho_{Ly}\right) + B_y(\theta,\phi)\left(1 + \frac{1}{\rho_{Lx}\rho_{Lx}}\right)}{1 - \left(\frac{\rho_{Ly}}{\rho_{Lx}}\right)}$$

## IV. Channel Balance Correction for Dual Polarized Probes

While dual polarized probes offer a 50% reduction in total test time, an extra level of complexity is introduced since they require the use of an RF switch to excite both ports. Even when a good RF switch is used, the amplitude and phase entering both ports of the probe will not be identical. This amplitude and phase imbalance should be measured and compensated for before transforming data to the far-field.

Here we make use of the same multi-point channel balance (MPCB) correction scheme presented in [3] and adapted from [4]. The on-axis ($\theta$ = 0°) fields for $\chi$ = 0°, 90° as a function of $\phi$ are compared and corrected. The MPCB technique relies on the fact that at $\theta$ = 0° the two $\phi$ cuts should radiate identical fields rotated by 90°. After de-rotation the fields can be compared and adjusted. A five-point MPCB correction procedure is used here, where fields are measured at ($\theta$,$\phi$) = (0,0), (0,90), (0,180), (0,270), (0,360) for both $\chi$ = 0°, 90°. Remember that for this case $\chi$ = 0° refers to port-1 of the probe, while $\chi$ = 90° refers to port-2 of the probe and that only the AUT is physically rotated. These imbalance factors are measured in advance and stored in a table containing amplitude/phase correction vs. frequency. Alternatively, the raw near-field data can be adjusted after the measurement is complete by analyzing the $\theta$ = 0° amplitude and phase data.

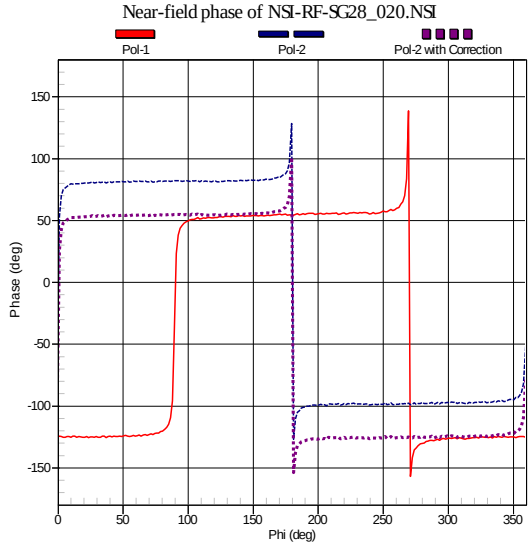


Figure 7 Near-field $\theta$ = 0° Polarization Cuts before and after 34° Correction Applied to $\chi$ = 90° Data

Figure 7 shows three $\theta$ = 0° near-field phase cuts as a function of $\phi$ rotation for a WR28 pyramidal gain horn at 26.5 GHz measured using a QRH probe. The first curve shows the $\chi$ = 0° (Pol-1) component. Next, we see the $\chi$ = 90° (Pol-2) component shifted along the x-axis by 90 degrees. While this is expected since the linear antenna is rotating as a function of $\phi$, there is an undesired bias along the Y-axis of roughly 34 degrees between the two curves. The probe has not been rotated, so this is a direct result of the two ports of the probe being excited with different phase. Using the MPCB correction routine, the phase is adjusted and the imbalance between the $\chi$ = 0° and $\chi$ = 90° components is nearly eliminated.

Figure 8 shows the main beam of the E-plane pattern for the same WR28 horn at 26.5 GHz. The first curve (WR28 Probe) was measured using a standard WR28 OEWG probe. The pattern is symmetric and smooth with a peak on-axis. Next, we see the results obtained using a QRH probe with no correction applied. A channel balance error of roughly 0.98 dB and 34° exists between the two ports of the probe and has a dramatic impact on the horn's main beam. Finally, when the MPCB correction factor is applied, we see excellent agreement between the WR28 and QRH probes.

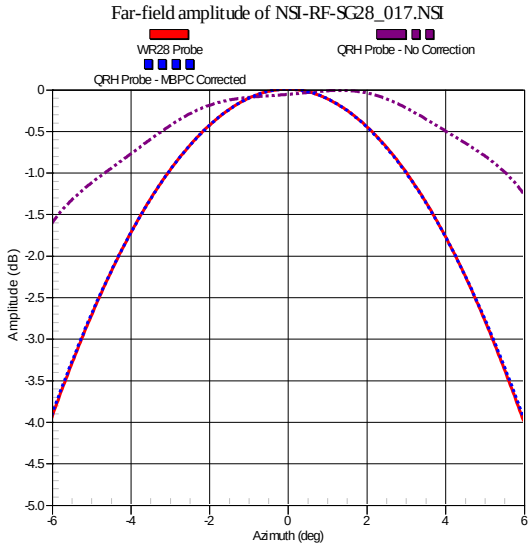


Figure 8. Far-Field E-Plane Cut Main Beam showing Effects of Channel Imbalance and Improvement using MPCB Algorithm

## V. Validating Probe Performance

At this point, the QRH probe has been characterized on the SNF system shown in Figure 5. From this characterization, probe pattern correction data was created. Now, when used as probe, the near-field to far-field transformation will be able to properly isolate the response of the AUT from the combined response of AUT and probe. The second port of the probe was also measured and polarization correction information was calculated and recorded. When this antenna is used as probe, this correction factor will be applied to the $\chi$ = 90° measured component. Finally, once mounted in the position of the probe, the MPCB procedure will be used

to determine and correct for the channel imbalance between the two ports of the probe.

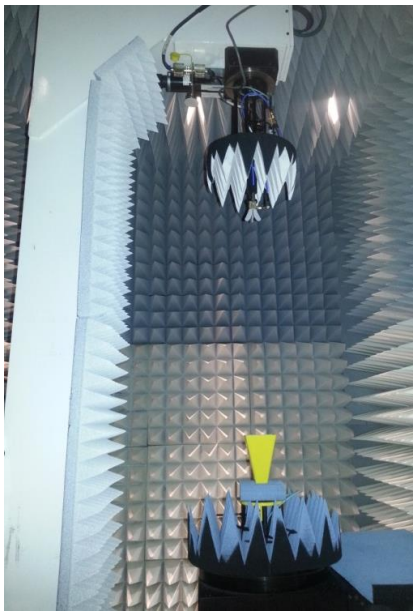

Figure 9. WR28 Standard Gain Horn Antenna Measured using WR28 OEWG Probe on NSI SNF Range

Using the same test system shown in Figure 5, some validation measurements were completed. First, a WR28 standard gain antenna was measured using an OEWG probe in the same band. Measurements were repeated with the QRH installed as probe, as shown in Figure 9. Figure 10 shows the on-axis cross-polarization level for three cases based on the validation measurements described here. With all three correction algorithms applied, we see very good cross-polarization agreement between the QRH and OEWG probes, with an average cross-polarization delta of 1.7 dB. However, when we ignore probe pattern correction for the QRH probe, the on-axis cross-polarization results deviate greatly from the trusted OEWG measurements, as much as 18 dB with an average of over 14 dB.

## VI. Conclusions

Building upon previous research, three correction algorithms were compiled and presented here. Probe pattern correction was shown to be of critical importance for broadband antennas where the patterns may vary significantly across their bandwidth. A polarization correction factor was presented that can be used to improve the performance achieved using dual polarized probes. Next, the simple MPCB correction scheme was shared along with some near-field and far-field results showing its effect. By combining probe pattern, polarization and channel balance correction schemes, an improvement to on-axis cross-polarization results for a WR28 SGH of roughly 12.3 dB was achieved when using a broadband QRH probe.

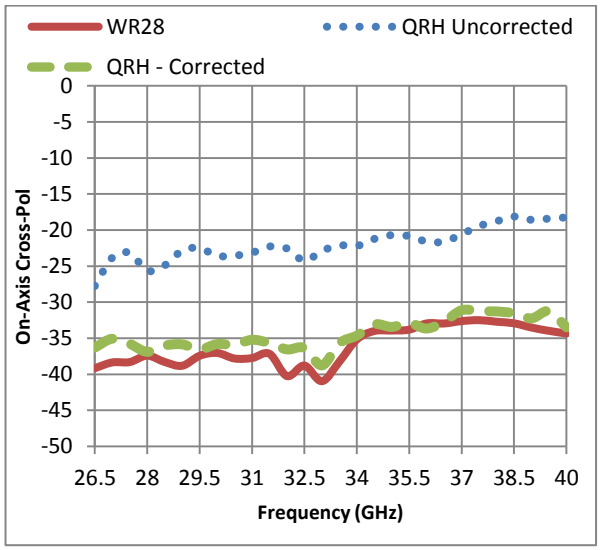


Figure 10 On-Axis Cross-Pol of WR28 Horn Measured with WR28 OEWG and QRH Probe with and without Correction

## References


[1] A.C. Newell, P. Pelland, "Measuring Low Cross Polarization Using a Broad Band, Log Periodic Probe" AMTA Annual Meeting & Symposium, 2012.

[2] P. Pelland, A.C. Newell, "Measuring Accurate Low Cross Polarization using Broad Band, Dual Polarized Probes", The Seventh European Conference on Antennas and Propagation (EuCap 2013) 8-12 April, 2013.

[3] P. Pelland, G. Hindman, A.C. Newell, "Advances in Automated Error Assessment of Spherical Near-Field Antenna Measurements", The Seventh European Conference on Antennas and Propagation (EuCap 2013) 8-12 April, 2013.

[4] Gregson S., McCormick J., Parini C., "Principles of Planar Near-Field Antenna Measurements", The Institute of Engineering and Technology, 2007. pp. 198-201.

[5] A.C. Newell, S. Gregson, "Estimating the Effects of Higher Order Modes in Spherical Near-Field Probe Correction", The Seventh European Conference on Antennas and Propagation (EuCap 2013) 8-12 April, 2013.

[6] A.C. Newell, "Error Analysis Techniques for Planar Near-Field Measurements", IEEE Transactions on Antennas and Propagation, AP-36, p. 581, 1988.

[7] G. Hindman, A.C. Newell, "Simplified Near-Field Accuracy Assessment", AMTA Annual Meeting & Symposium, 2006.

[8] P. Pelland, J. Ethier, D. J. Janse van Rensburg, D. A. McNamara, L.Shafai & S. Mishra, "Towards Routine Automated Error Assessment in Antenna Spherical Near-field Measurements", The Fourth European Conference on Antennas and Propagation (EuCap 2010) 12-16 April, 2010.

[9] G. Hindman, D.S. Fooshe, "Probe Correction Effects on Planar, Cylindrical and Spherical Near-Field Measurements", AMTA Annual Meeting & Symposium, 1998.

[10] A.C. Newell, G. Hindman, "Quantifying the Effects of Position Errors in Spherical Near-Field Measurements", AMTA Annual Meeting & Symposium, 1998.